Received: 6 February 2020 | Accepted: 7 June 2020

DOI: 10.1002/jcp.29885

ORIGINAL RESEARCH ARTICLE

Journal of Cellular Physiology WILEY

Absence of the MFG-E8 gene prevents hypoxia-induced pulmonary hypertension in mice

Jun Wang[1,2] | Jixing Wu[1] | Xianying Zhu[1] | Jinkun Chen[3] | Jianping Zhao[1] | Yongjian Xu[1] | Jungang Xie[1]

[1]Department of Respiratory and Critical Care Medicine, National Clinical Research Center of Respiratory Disease, Key Laboratory of Pulmonary Diseases of Health Ministry, Tongji Hospital, Tongji Medical College, Huazhong University of Science and Technology, Wuhan, Hubei, China

[2]Department of Rheumatology and Immunology, Beijing Chaoyang Hospital of Capital Medical University, Beijing, China

[3]St. John's-Ravenscourt School, Winnipeg, MB, Canada

Correspondence
Jungang Xie, Department of Respiratory and Critical Care Medicine, National Clinical Research Center of Respiratory Disease, Key Laboratory of Pulmonary Diseases of Health Ministry, Tongji Hospital, Tongji Medical College, Huazhong University of Science and Technology, Wuhan, 430030 Hubei, China.
Email: xiejjgg@hotmail.com

Funding information
National Key R&D Program of China, Grant/Award Numbers: 2016YFC1304500, 2018YFC1311900; National Natural Science Foundation of China, Grant/Award Numbers: 81370145, 81570033, 81973986; National Key Basic Research and Development Program (973 program), Grant/Award Number: 20I5CB553403

Abstract

Pulmonary hypertension (PH) is a chronic vascular disease characterized by elevated pulmonary arterial resistance and vascular remodeling, and chronic hypoxia plays an important role in PH. Milk fat globule-EGF factor 8 (MFG-E8) is a glycoprotein that regulates cell proliferation and apoptosis, but its role in hypoxia-induced PH is unknown. The current study aimed to determine the function and fundamental mechanisms of MFG-E8 in hypoxia-induced PH. Herein, we exposed mice to hypoxia for 5 weeks, and MFG-E8 was found to be elevated in mouse lung tissues, arteries, and plasma. Compared with wild-type littermates, mice lacking MFG-E8 showed a significant increase in the ratio of pulmonary artery acceleration time to ejection time (PAT/PET), while they showed decreases in right ventricular systolic pressure, the Fulton's Index, percent medial wall thickness (%WT), and vascular muscularization in pulmonary arteries. In addition, MFG-E8 protein levels were also increased in the serum of patients with chronic PH. Similarly, we observed a higher expression of MFG-E8 in human pulmonary artery smooth muscle cells (PASMCs) in the presence of hypoxic stimulation than MFG-E8 in cells in normoxic conditions. Furthermore, MFG-E8 silencing resulted in partial inhibition of proliferation, migration and cell cycle progression in human PASMCs, and the possible mechanisms might involve the interaction between MFG-E8 and the p-Akt/cyclin D1 pathway. Collectively, our study suggests that the absence of MFG-E8 can attenuate the development of hypoxia-induced PH and vascular remodeling. MFG-E8 can be a potential therapeutic target or a biomarker for PH.

KEYWORDS

hypoxia, MFG-E8, pulmonary artery smooth muscle cells, pulmonary hypertension, pulmonary vascular remodeling

Jun Wang and Jixing Wu contributed equally to this study.

1 | INTRODUCTION

Pulmonary hypertension (PH) is a pulmonary vasculature disease characterized by progressive elevations in pulmonary artery (PA) pressure and vascular remodeling, which eventually leads to right ventricular hypertrophy and heart failure that can threaten patient health and survival (Barman et al., 2019; Bogaard, Abe, Vonk Noordegraaf, & Voelkel, 2009; Udjus et al., 2019). Chronic hypoxia triggers PH and plays an important role in its development. People living at high altitudes presented increased PA vascular resistance (Arias-Stella & Saldana, 1963; Blissenbach et al., 2018). Lung diseases involved in alveolar hypoxia, such as chronic obstructive pulmonary disease (COPD), interstitial lung disease (ILD) and obstructive sleep apnea (OSA), were commonly associated with PH formation (Naeije, 2005; Sajkov & McEvoy, 2009; Strange & Highland, 2005). Meanwhile, it has been reported that chronic hypoxia stimuli caused right ventricular hypertrophy and vascular remodeling in animals (Beloiartsev et al., 2015), of which hypertrophy and hyperplasia, as well as migration of the pulmonary artery smooth muscle cells (PASMCs), are key pathologic features that contribute to the thickening of the vascular medial layer (Jeffery & Wanstall, 2001; Stenmark, Fagan, & Frid, 2006).

Milk fat globule-EGF factor 8 (MFG-E8), also known as Mfge8 or lactadherin, is a lipophilic glycoprotein secreted by the mammary gland, and it was first identified on the surface of milk fat globule membranes (Oshima, Aoki, Kato, Kitajima, & Matsuda, 2002). Structurally, the mouse MFG-E8 essentially contains two repeated N-terminal EGF-like domains and two repeated C-terminal EGF-like domains with homology to coagulation factors V and VIII (Aziz, Jacob, Matsuda, & Wang, 2011). Previous studies found protein expression in several types of cells, including macrophages, dendritic cells and carcinoma cells (Raymond, Ensslin, & Shur, 2009). It has been proven that MFG-E8 participates in a range of cellular functions, such as mediating sperm-egg binding (Shur, Ensslin, & Rodeheffer, 2004), triggering clearance of apoptotic cells (Hanayama et al., 2004), and promoting neovascularization (Silvestre et al., 2005).

Recent studies reported that MFG-E8 has roles in vascular diseases, in which protein expression was increased in possible association with arterial remodeling in atherosclerosis or angiopathy in diabetes (Bagnato et al., 2007; Beauchamp, van Achterberg, Engelse, Pannekoek, & de Vries, 2003; B. Li et al., 2011). Lin et al. (2010) found that MFG-E8 was enriched not only in the aortic walls of renal hypertensive rats but also in the serum of hypertensive patients with chronic renal failure. Meanwhile, treatment of aged rat aortic vascular smooth muscle cells (VSMCs) with recombinant human MFG-E8 could facilitate cell proliferation via integrin/ERK1/2/cyclin-dependent kinase 4 (CDK4)/PCNA signaling pathways, whereas MFG-E8 silencing depressed VSMC cell cycle progression and cell proliferation (Wang et al., 2012).

Together, the above studies indicate that MFG-E8 participates in vascular remodeling in some diseases. However, the pivotal role of MFG-E8 in PH has not been elucidated. Hence, we hypothesized that MFG-E8 expression would change and regulate PH progression. We used a murine model of chronic hypoxia-induced PH to assess the difference in PA pressure and vascular remodeling between MFG-E8 transgenic mice and wild-type littermates. MFG-E8 measurements were also taken from patients with PH. From the in vitro studies, we examined MFG-E8 expression in human PASMCs under hypoxic stimulation and preliminarily explored whether MFG-E8 could alter cell proliferation and migration, therefore influencing vascular remodeling.

Our data indicated that chronic hypoxia-induced MFG-E8 expression elevation in both the lung, pulmonary arteries, and plasma of mice, and consistent results were observed in PH patient serum and PASMCs. The absence of MFG-E8 attenuated the extent of PH and vascular remodeling, possibly through alleviating PASMC remodeling accompanied by P-AKT and cyclin D1 alterations.

2 | MATERIALS AND METHODS

2.1 | Animals

All animal experiments were approved by the Institutional Animal Care and Use Committee of Tongji Medical College (Wuhan, China), Huazhong University of Science and Technology. Mice with a heterozygous MFG-E8 genotype were chosen as the parental generation (genetic background of C57BL/6, which were generous gifts from Professor Tianpen Cui, Laboratory of Clinical Immunology, Wuhan No. 1 Hospital). The gene knockout procedure was performed as previously described (Huang et al., 2017). The genotypes of the offspring were determined by genomic DNA analysis, assessment of mouse tail biopsy samples (Figure 1) and real-time PCR detection of the RNA extracted from lung tissues. The list of primers used for MFG-E8 gene identification is displayed in Table S1. Wild-type (MFG-E8$^{+/+}$) and transgenic (MFG-E8$^{-/-}$) male mice were used for experiments.

2.2 | Patients and controls

For these investigations, 35 male patients with PH and 30 healthy male volunteers who were admitted to Tongji Hospital (Wuhan, China) between April 1 and August 12, 2019, were recruited. The primary etiologies for these PH patients included a diagnosis of PAH (WHO group 3) according to international diagnostic criteria (Simonneau et al., 2013), such as COPD, obstructive sleep apnea syndrome (OSAS) and ILD, and so forth while COPD accounted for more percentage. The exclusion criteria included left ventricular systolic or diastolic dysfunction, hypertension, coronary heart disease, diabetes mellitus, autoimmune diseases, malignancy, infections, severe endocrine, hepatic, or renal diseases, and medical treatment, including corticosteroids or immunosuppressive agents (Joppa, Petrasova, Stancak, & Tkacova, 2006; Olsson et al., 2016; Rohm et al., 2017; Song et al., 2018). The 10 patients accepted right heart catheterization, the mean pulmonary artery pressure (mPAP) max/min value was 73/35 mmHg, and the pulmonary artery wedge pressure value for all of the 10 people was less than 15 mmHg. All the two groups undertook the echocardiography

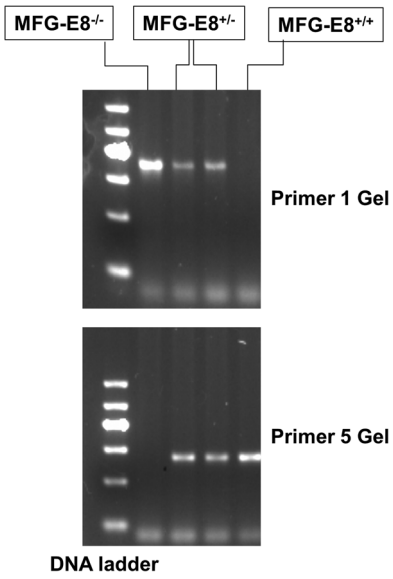

FIGURE 1 *MFG-E8* gene identification in C57BL/6 mice. Mouse DNA was acquired from the tail and was extracted by a genome DNA kit. The amplification product from the polymerase chain reaction was analyzed via gel electrophoresis imaging to determine the genotype. Both Primer 1 and Primer 5 were used to distinguish between different genotypes. Knockout mice (MFG-E8$^{-/-}$) only expressed the Primer 1 allele, whereas wild-type mice (MFG-E8$^{+/+}$) only expressed the Primer 5 allele, and the heterozygous mice (MFG-E8$^{+/-}$) expressed both Primer 1 and Primer 5. MFG-E8, milk fat globule-EGF factor 8

examination, the value of the pressure gradient tricuspid valve regurgitation, PGTI, was greater than 45 mmHg in PH patients. Blood serum samples were collected and stored at −80°C for further study. All patients and volunteers signed written informed consent, and the Ethics Committee of Tongji Hospital approved this study.

2.3 | Chronic exposure to hypoxia

A murine model of PH induced by chronic hypoxia was established as previously described (Ball et al., 2014). Briefly, male mice (aged 8–10 weeks, 20–25 g) were randomly placed in either a hypoxic chamber (a mixture of room air and nitrogen with the oxygen concentration maintained at 10% as monitored by an oxygen detector) or a normoxic chamber (21% oxygen concentration) for 5 weeks (Hu et al., 2019; Novoyatleva et al., 2019; Xiao, Gong, & Wang, 2013). Then, the hemodynamic parameters and morphologic tissue measurements of mice were analyzed, while blood samples, as well as lung and pulmonary arteries, were processed for further examinations.

2.4 | Echocardiographic and hemodynamic measurements

The hemodynamic parameters of the mice were assessed by two methods. Animals were anesthetized by inhalation of isoflurane, and a VEVO Doppler ultrasound imaging system (VisualSonics, Toronto, ON) was used to detect and record images for the determination of pulmonary artery acceleration time (PAT), pulmonary artery ejection time (PET) and other parameters as indicated. Later, the right ventricular systolic pressure (RVSP) was measured via a PowerLab system (ADInstruments, Australia) as previously described (Chu, Xiangli, & Xiao, 2015; van Suylen, Aartsen, Smits, & Daemen, 2001). Briefly, the animals were anesthetized with intraperitoneal sodium pentobarbital (80 mg/kg) and treated with tracheal intubation. A 26-G needle (Sigma-Aldrich, St. Louis, MO) connected with a pressure transducer was used to puncture into the right ventricular cavity. Data recording began after a stable tracing waveform was achieved.

2.5 | Blood plasma

Animals were killed after their hemodynamic parameters were measured, and blood samples were collected in anticoagulant tubes and centrifuged at 3,000 rpm for 5 min. Plasma and blood cells were separated and stored at −80°C.

2.6 | Sample processing and assessment of right ventricle hypertrophy

Hearts, lungs, and connected vessels were isolated from the chest cavity of mice, and the main pulmonary artery was carefully dissected. Arteries were washed in normal saline and stored at −80°C. The left lungs were fixed in 4% paraformaldehyde for further analysis, and the right lungs were stored at −80°C. The right ventricle (RV) was dissected from the left ventricle and interventricular septum (LV + S). RV hypertrophy was assessed by the weight ratio of RV to (LV + S) and was expressed as Fulton's index.

2.7 | Morphologic analysis of pulmonary arteries

Through paraformaldehyde fixation and dehydration, the paraffin-embedded left lungs were cut into 4-μm-thick sections, and they were stained with hematoxylin and eosin (HE) or Masson's trichrome. For HE staining of lung tissues, the percent wall thickness (%WT) was calculated for evaluating pulmonary vascular remodeling. All oval or round pulmonary arteries with an external diameter of 25–100 μm were assessed under a ×400 microscope (Olympus BX61, Tokyo, Japan). The images were analyzed using Image-pro plus 6.0 (Media Cybernetics, MD). The %WT was calculated as previously described (Q. Li et al., 2017) to assess pulmonary vascular remodeling: %WT = [(external diameter − internal diameter)/external diameter] × 100%. Additional evaluation of vascular remodeling was performed by immunohistochemical staining with α-smooth muscle actin (α-SMA; Abcam, Cambridge, UK). All pulmonary arteries with an external diameter less than 50 μm were identified, and arterial muscularization was assessed. As previously described (Ball et al., 2014),

nonmuscularized vessels were defined as having less than 25% of vessel circumference having visible staining by α-SMA, while fully muscularized vessels were completely stained with α-SMA, and partially muscularized vessels were falling in between those two groups. The images were scanned and analyzed using a Pannoramic MIDI (3Dhistech, Budapest, Hungary) with an enlargement of ×400.

2.8 | Quantitative real-time PCR

Total RNA was extracted from mouse lungs or human PASMCs and was used to generate cDNA using reverse-transcription PCR (RT-PCR) with a first-strand cDNA reverse-transcription kit (Takara, Dalian, China). Quantitative real-time PCR was performed using an SYBR Green PCR Master Mix (Takara) and a 7500 Real-Time PCR System (Applied Biosystems, Thermo, Waltham, MA).

The primer pairs used for amplification were as follows: mouse β-actin, forward, 5′-TGCTGTCCCTGTATGCCTCT-3′; reverse, 5′-TTG ATGTCACGCACGATTTC-3′; mouse MFG-E8: forward, 5′-AACAAC CTAGCCTCCCGTTG-3′; reverse, 5′-TGTCCAGGCATTGACGATCC-3′; human β-actin: forward, 5′-CCTCGCCTTTGCCGATCC-3′; reverse, 5′-GGATCTTCATGAGGTAGTCAGTC-3′; and human MFG-E8: forward, 5′-CCTGCCACAACGGTGGTTTAT-3′; reverse, 5′-GCGATCTG TGAGTTGGCAATGT-3′.

2.9 | Western blot analysis

Total tissues or cell lysates were extracted from mouse lungs, pulmonary arteries, and human PASMCs; protein concentrations were determined using a BCA kit (Aspen, Wuhan, China). Whole lysates were separated by sodium dodecyl sulfate-polyacrylamide gel electrophoresis and were then transferred onto PVDF membranes, which were blocked with 5% BSA in Tris-buffered saline containing 0.5% Tween-20 for 1 hr at room temperature. The membranes were then incubated with primary antibodies overnight at 4°C before they were reacted with HRP-conjugated secondary antibodies. An ECL reagent was used for chemiluminescent detection, and the membranes were analyzed using the ChemiDoc MP System (BioRad Laboratories, CA). Band intensities were quantitatively measured using ImageJ (NIH, Bethesda, MD). Primary antibodies against β-actin (TDY Biotech Co., Beijing, China), mouse MFG-E8 (R&D Systems, Minneapolis, MN), human MFG-E8 (Abcam), p-AKT, AKT (Cell Signaling Technology, Danvers, MA) and cyclin D1 (Proteintech Group Inc., Wuhan, China) were used.

2.10 | Enzyme-linked immunosorbent assay (ELISA) detection of MFG-E8 levels

Levels of MFG-E8 in mouse plasma, human serum or PASMC cultured supernatants were measured using a Quantitative ELISA Kit (R&D Systems, Minneapolis, MN) according to the manufacturer's instructions. Absorbance was measured at 450 nm and was recorded (PerkinElmer, Waltham, MA).

2.11 | Human PASMC culture

Primary human PASMCs were purchased from ATCC (MD) and were identified by immunofluorescence staining of α-SMA as described previously (Q. Li et al., 2017). Cells were cultured in DMEM-F12 medium (HyClone, Logan, UT) containing 10% fetal bovine serum (FBS; Gibco, Australia), and streptomycin and penicillin at 37°C in a 5% carbon dioxide/95% air environment; 2% oxygen stimulation was given for the hypoxia group. Passages 4 through 6 were used for further experiments. Cells were incubated overnight with 2% FBS for synchronization before the intervention.

2.12 | Immunofluorescence

Human PASMCs were cultured and stimulated, fixed in 4% paraformaldehyde, permeabilized with phosphate buffered saline (PBS) containing 0.1% Triton-X and blocked with blocking buffer. Cells were incubated with the primary antibody against MFG-E8 (Abcam) and FITC-conjugated anti-mouse IgG (Jackson ImmunoResearch, West Grove, PA), with subsequent washing to remove the nonspecific binding. Cell nuclei were stained with 4′,6-diamidino-2-phenylindole (DAPI). Positively stained cells were observed by confocal laser scanning Immunofluorescence microscopy (Nikon, Tokyo, Japan).

2.13 | Small RNA interference

Human PASMCs (30–50% confluence) were transfected with small interfering RNA (siRNA) using a Lipo2000 transfection reagent (Invitrogen, Carlsbad, CA) according to the manufacturer's protocol. MFG-E8 siRNA sequences were: 5′–3′ GCCUGAAGAAUAAC AGCAUTT, and 5′–3′ AUGCUGUUAUUCUUCAGGCTT; negative control (NC) siRNA sequences were: 5′–3′ UUCUCCGAACGUGUC ACGUTT, and 5′–3′ ACGUGACACGUUCGGAGAATT. MFG-E8 mRNA was detected by quantitative real-time PCR after 24 hr. For another 24 hr, cells were lysed for western blots and their supernatants were collected for ELISA analysis to evaluate transfection efficiency.

2.14 | CCK8 assay and cell cycle analysis

To investigate the effect of MFG-E8 on the proliferation of human PASMCs, cells were seeded in 96-well plates, treated with siRNA interference after serum starvation, then placed in an incubator of 2% or 21% oxygen for 48 hr. Cell proliferation was determined using a CCK8 kit (Promotor, Wuhan, China) according to the manufacturer's instructions. Absorbance was measured at 450 nm and recorded (PerkinElmer, Waltham, MA).

Cells were harvested with trypsin, fixed for 16 hr with 75% ethanol and then centrifuged. Cold PBS (1 ml) was used to wash the cells. A Cell Cycle Detection Test Kit (KeyGen Biotech, Nanjing, China) was used to stain cells with propidium iodide and RNase A, according to the manufacturer's instructions. Cell cycle experiments were performed using a flow cytometer (FACSCalibur, Becton, Dickinson and Company, Franklin Lakes, NJ). All experiments were independently performed in triplicate.

2.15 | Cell apoptosis analysis

Human PASMCs were seeded on six-well plates and exposed to hypoxia and/or MFG-E8 siRNA stimulation. Then, the cells were harvested with trypsin, and the apoptotic cells stained with a PI/annexin V-FITC kit (KeyGen Biotech) according to the manufacturer's instructions and were measured with a flow cytometer (Becton, Dickinson and Company). All experiments were independently performed in triplicate.

2.16 | Transwell assay

Membranes with 8-μm pores (Corning Costar, Cambridge, MA) in 24-well Transwell® plates were employed for migration assays. PASMCs were transfected with MFG-E8 siRNA for 24 hr before being digested and counted. Approximately 50,000 cells were added to the upper chamber for 24 hr to adhere. Next, the medium in the upper chamber was replaced with 200 μl of fresh complete medium containing 2% FBS, and 600 μl of standard culture medium with 15% FBS was added to the lower compartment. After 24 hr, the cells in the membranes of the bottom chambers were fixed, stained with 0.1% crystal violet and imaged. All experiments were independently performed in triplicate.

2.17 | Statistical analysis

The data were statistically analyzed with GraphPad Prism 5.0 software (San Diego, CA) and SPSS Statistics 19 (IBM, NY). Values were fitted to a normal distribution and are represented as the mean ± standard error of the mean (*SEM*). Comparisons between two groups were performed using Student's *t* tests. For multiple comparisons, normally distributed data were analyzed using one-way analysis of variance followed by Newman–Keuls tests. A $p < .05$ was considered statistically significant.

3 | RESULTS

3.1 | Chronic hypoxia exposure stimulated MFG-E8 expression in vivo

An in vivo study demonstrated that hypoxia exposure upregulated MFG-E8 expression in mice (Figure 2). The protein was increased both in lung tissues and the main pulmonary arteries in mice that were exposed to chronic sustained hypoxia; nonetheless, the transgenic littermates showed no detectable MFG-E8 expression (Figure 2a,c). Our results indicated a significant difference between the normoxia group and the hypoxia group (Figure 2b,d). Meanwhile, as measured by the ELISA kit, hypoxia stimulation resulted in a higher value of secreted MFG-E8 in mouse plasma than what was observed in the control group (Figure 2e, 3.37 ± 0.19 ng/ml vs. 2.63 ± 0.21 ng/ml, $p < .05$).

3.2 | MFG-E8 serum concentrations in PH patients

This study enrolled 35 PH patients and 30 healthy volunteers. The baseline characteristics of the PH patients and controls, are shown in Table 1. There was no significant difference in age, body mass index (BMI) or blood pressure between the two groups. MFG-E8 serum concentrations were quantified by an ELISA kit and were found to be significantly elevated in the PH patient group (shown in Figure 2f, 2,794 ± 165 pg/ml, 2.79 ± 0.16 ng/ml) compared with the control group (2,136 ± 154 pg/ml, 2.14 ± 0.15 ng/ml).

3.3 | Hypoxia-induced MFG-E8 expression in human PASMCs

To test whether hypoxia would affect MFG-E8 expression in vitro, human PASMCs were cultured in a hypoxic environment for 48 hr or 72 hr and were then analyzed by western blot or cell immunofluorescence staining (Figure 3). The western blot results indicated a significant increase in MFG-E8 after hypoxic stimulation (Figure 3a–d), and the qualitative immunofluorescence also showed a difference (Figure 3e). The amount of MFG-E8 in PASMC supernatants, indicative of secreted MFG-E8 (Figure 3f), was much higher in the hypoxia group (42,980 ± 1,368 pg/ml, 42.98 ± 1.37 ng/ml) than in the normoxia group (27,980 ± 623 pg/ml, 27.98 ± 0.62 ng/ml).

3.4 | Evaluation of pulmonary hemodynamics in mice

A murine model of PH was established by treating mice to hypoxia stimulating conditions by exposing them to continuous 10% O_2 for 5 weeks. Pulmonary hemodynamics were assessed by echocardiography and by measurement of the RVSP. In the normoxic environment, wild-type and MFG-E8$^{-/-}$ mice had similar hemodynamic parameters, as evidenced by the lack of significant differences in PAT, ratio of pulmonary artery acceleration time to pulmonary artery ejection time (PAT/PET), and RVSP (Figure 4a–e). Compared with the normoxia group, the 10% O_2 WT group showed an apparent decrease in the PAT/PET value (0.21 ± 0.01 vs. 0.32 ± 0.01) and an increase in the RVSP value (33.12 ± 1.06 vs. 23.48 ± 0.98 mmHg). However, MFG-E8-null mice exposed to hypoxia showed significantly

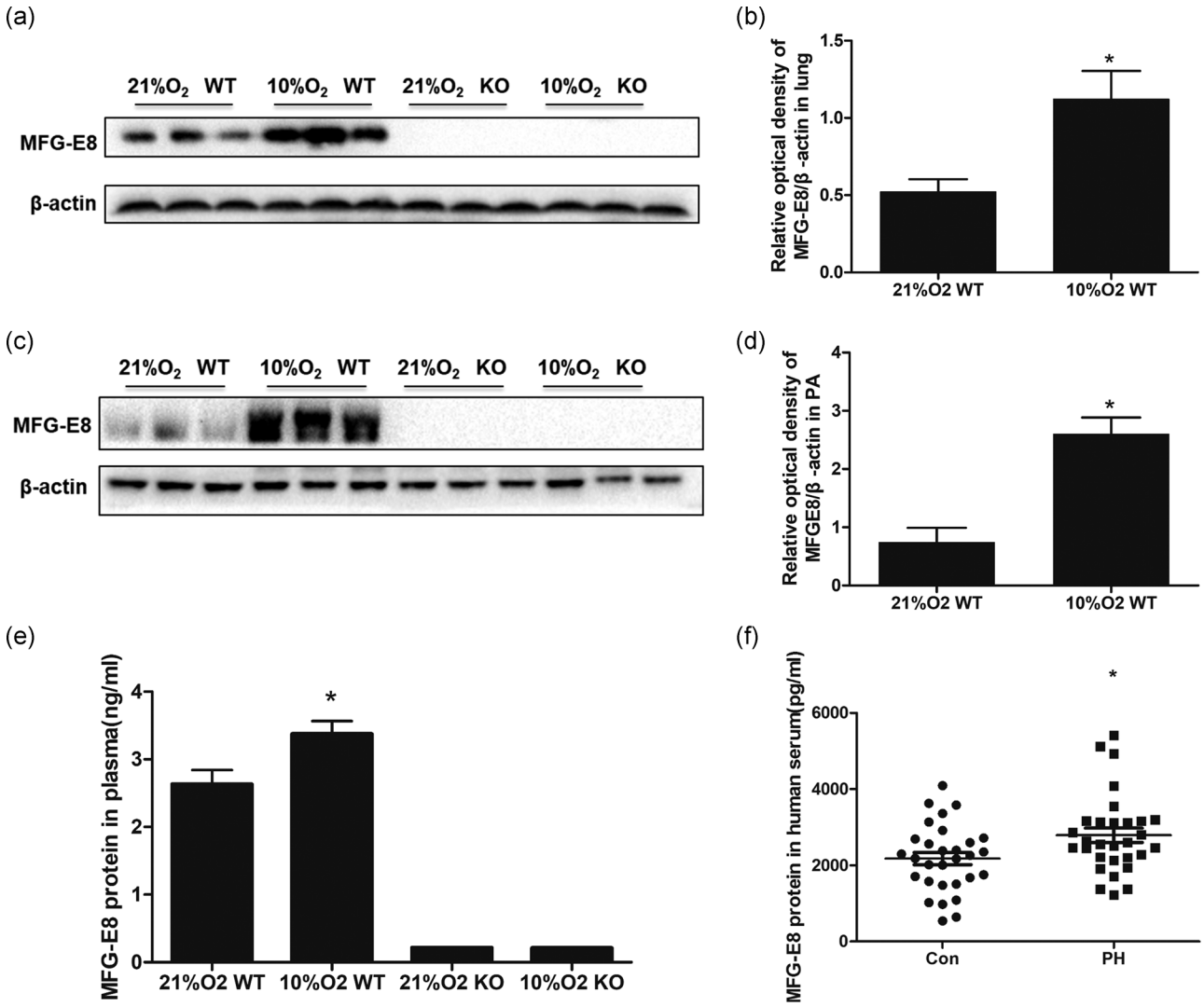

FIGURE 2 MFG-E8 protein expression in chronic hypoxia-induced mice and PH patients. Representative western blot images of MFG-E8 in lung (a) and average data (b). Representative western blots in pulmonary arteries (c) and average data (d), $n = 3$. (e) ELISA detected the MFG-E8 protein in mouse blood plasma (ng/ml); $n = 6$; $^*p < .05$ compared with the 21% O_2 WT group. (f) MFG-E8 protein in human blood serum (pg/ml); $n = 30$ or 35, results are expressed as the mean ± *SEM*, and $^*p < .05$ compared with the control group. ELISA, enzyme-linked immunosorbent assay; KO, knockout; MFG-E8, milk fat globule-EGF factor 8; PH, pulmonary hypertension; WT, wild type

higher PAT/PET values (0.25 ± 0.01 vs. 0.21 ± 0.01) as well as lower RVSP values (28.36 ± 1.15 vs. 33.12 ± 1.06 mmHg) compared with the 10% O_2 WT group. Measurements of left ventricular function by echocardiography technology revealed no significant changes in the left ventricular shortening fraction (LV-FS) and left ventricular ejection fraction (LV-EF) among the four groups (Table 2), suggesting that chronic hypoxia did not affect left ventricular function.

3.5 | Assessment of right ventricular hypertrophy and pulmonary vascular remodeling

The weight ratio of the right ventricle to the left ventricle plus septum (RV/(LV+S)) is a measurement used to assess RV hypertrophy. Hypoxia stimulation induced significant RV hypertrophy compared with the normoxia group. However, after exposure to

TABLE 1 Baseline characteristics of pulmonary hypertension (PH) patients and controls

Group	Controls ($n = 30$)	PH patients ($n = 35$)	p value
Age (years)	57 ± 2	61 ± 3	ns
Body mass index (kg/m^2)	23.5 ± 1.1	24.9 ± 1.3	ns
Systolic blood pressure (mmHg)	133 ± 3	137 ± 5	ns
Diastolic blood pressure (mmHg)	72 ± 4	69 ± 3	ns

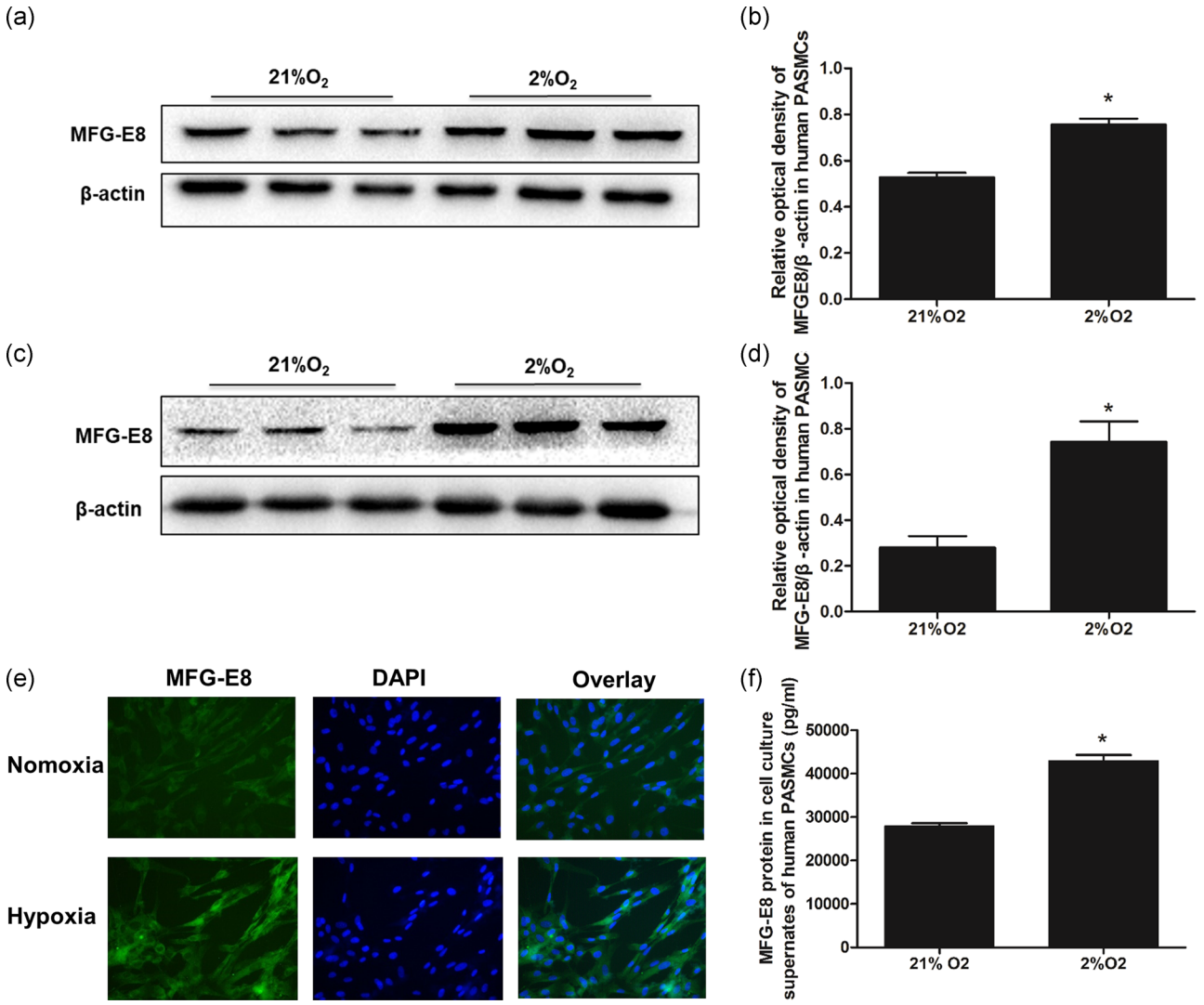

FIGURE 3 MFG-E8 protein expression in human PASMCs. Representative western blot images of MFG-E8 (a) and average data (b) after 48 hr of exposure to 2% O_2. Representative western blots of MFG-E8 (c) and average data (d) after 72 hr of exposure to 2% O_2; $^*p < .05$ compared with 21% O_2. (e) Qualitative immunofluorescence staining for MFG-E8 (green) and nuclei (DAPI) after 48 hr of exposure to 2% O_2. (f) ELISAs detected MFG-E8 protein in collected human PASMC cultured supernatants (pg/ml); $n = 3$, results are expressed as the mean ± *SEM*, and $^*p < .05$ compared with the 21% O_2 group. DAPI, 4′,6-diamidino-2-phenylindole; ELISA, enzyme-linked immunosorbent assay; MFG-E8, milk fat globule-EGF factor 8; PASMC, pulmonary artery smooth muscle cell

chronic hypoxia, the RV/(LV+S) value for MFG-E8$^{-/-}$ mice was significantly lower than it was in the MFG-E8$^{+/+}$ mice (Figure 4f).

The percent wall thickness (WT%) of pulmonary arteries was measured to evaluate pulmonary vascular remodeling. Although wild-type and transgenic mice showed a significant increase in WT% following exposure to continuous hypoxia, an alleviation of vascular remodeling was found in transgenic mice compared with their littermates (Figure 4g,h). Abnormal deposition of the extracellular matrix (ECM) is also a part of pulmonary vascular remodeling, and collagen is the main component of ECM. The Masson staining results showed that the absence of MFG-E8 could partially inhibit chronic hypoxia-induced ECM deposition (Figure 4i).

In addition, assessment of distal arteriole muscularization was performed for further remodeling estimation (Figure 4j,k). There was no difference in the percentages of nonmuscularized, partially muscularized and fully muscularized vessels between the two normoxia groups. Chronic hypoxia stimulation significantly increased the distal pulmonary artery muscularization, while MFG-E8 null mice exposed to hypoxia exhibited some amount of alleviation. These results were consistent with the observed changes in pulmonary hemodynamics and right ventricular hypertrophy.

3.6 | Detection of MFG-E8 interference efficiency

Human PASMCs were transfected with MFG-E8 small interfering RNA (siRNA), and the mRNA and protein levels of MFG-E8 were assessed by RT-PCR, western blot and ELISA. Transfection with

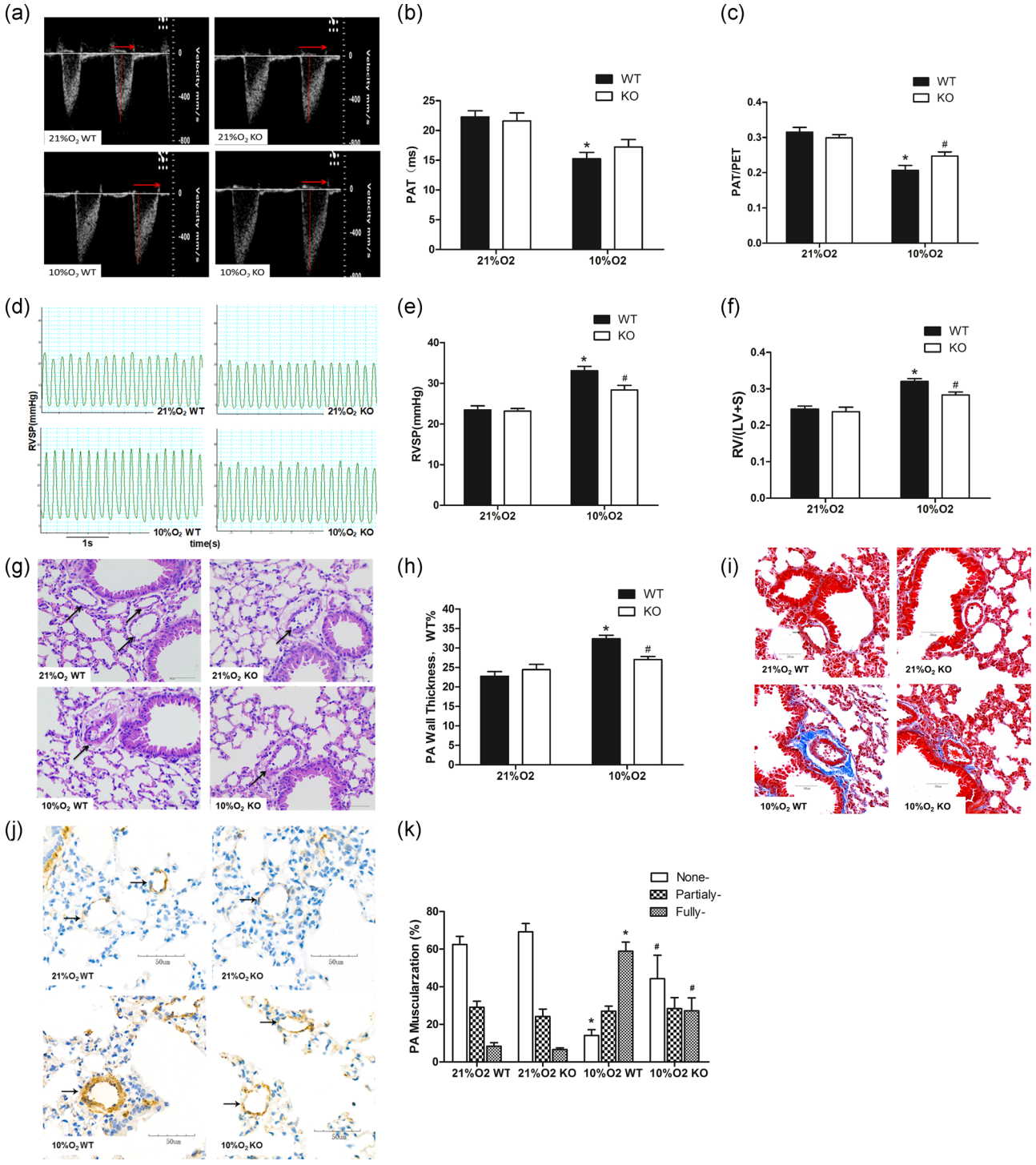

FIGURE 4 *MFG-E8* gene knockout and pulmonary hypertension induced by chronic hypoxia in mice. (a) Representative pulse-wave doppler images across the pulmonary outflow tract. The time to peak flow acceleration across the pulmonary valve decreases with increasing pulmonary artery pressure, and the ratio of PAT/PET varies and is inverse to pulmonary artery pressure. (b,c) PAT and PAT/PET demonstrated that pulmonary artery resistance increased by chronic hypoxia and is alleviated in the MFG-E8 knockout; $n = 6$. (d) Representative RVSP images showing that pulmonary vascular resistance differed between the four groups. (e) RVSP alteration in *MFG-E8* gene knockout and/or chronic hypoxia-induced mice; $n = 6$. (f) Changes in Fulton's index, and the ratio of right ventricular to left ventricular plus septal weight, RV/(LV + S), in four groups of mice; $n = 6$. (g) Representative hematoxylin and eosin-stained mouse lung tissue sections showed vascular remodeling in small pulmonary arteries. (h) Quantification of wall thickness (WT%) indicated attenuated vascular remodeling in MFG-E8$^{-/-}$ mice; $n = 6$. (i) Representative Masson staining of collagen deposition around mouse pulmonary arteries. (j) Representative α-sma stained distal pulmonary arteries indicated vascular muscularization differences between the four groups. (k) Chronic hypoxia-induced distal muscularization, while MFG-E8 null mice showed an alleviation of the muscularization; $n = 5–6$. The results are expressed as the mean ± *SEM*, $^{*}p < .05$ compared with the 21% O_2 WT group, and $^{\#}p < .05$ compared with the 10% O_2 WT group. KO, knockout; MFG-E8, milk fat globule-EGF factor 8; NC, negative control; PAT/PET, pulmonary acceleration time to total pulmonary ejection time; RVSP, right ventricular systolic pressure; WT, wild type

TABLE 2 Major data of mice for echocardiography measurement

Group	PAT (ms)	PET (ms)	PAT/PET	LV-EF (%)	LV-FS (%)
21% O_2 WT	22.28 ± 1.03	70.37 ± 2.60	0.32 ± 0.01	56.51 ± 2.30	29.18 ± 1.50
10% O_2 WT	15.24 ± 1.09*	73.96 ± 3.48	0.21 ± 0.01*	60.30 ± 4.16	31.90 ± 2.70
21% O_2 KO	21.62 ± 1.33	72.39 ± 3.76	0.30 ± 0.01	57.02 ± 1.89	29.47 ± 1.24
10% O_2 KO	17.21 ± 1.26	69.24 ± 2.18	0.25 ± 0.01#	57.61 ± 3.14	29.84 ± 1.99

Abbreviations: KO, knockout; LV-EF, left ventricular ejection fraction; LV-FS, left ventricular shortening fraction; PAT, pulmonary artery acceleration time; PET, pulmonary artery ejection time; WT, wild type.

MFG-E8 siRNA resulted in a significant decrease in MFG-E8 mRNA and protein expression, and the amount of MFG-E8 in cell supernatants also showed an apparent decrease (Figure 5a–c).

3.7 | MFG-E8 silencing attenuated human PASMC cell cycle progression and proliferation

To further explore the roles of MFG-E8 in PASMCs, we silenced MFG-E8 expression and used a CCK8 assay to measure cell proliferation (Figure 5d). MFG-E8 silencing apparently decreased the number of cells identified by CCK8 and partially attenuated hypoxia-induced cell proliferation. We next determined whether MFG-E8 silencing would affect cell cycle progression (Figure 5e–g). Hypoxia stimuli-associated cell numbers that were increased in the S phase and decreased in G0/G1 were inhibited by pretreatment with MFG-E8 siRNA. Meanwhile, a single application of MFG-E8 siRNA resulted in a significantly decreased number of S phase cells, which was consistent with the changes observed in the CCK8 assay. Additionally, the number of apoptotic cells (Figure 5h) showed no significant alterations following either hypoxia stimulation or MFG-E8 siRNA treatment. Together, these data revealed that MFG-E8 silencing partially eliminated the hypoxia-induced promotion of cell cycle progression and cell proliferation.

3.8 | MFG-E8 silencing attenuated human PASMC migration

Transwell assays were applied to measure the PASMC migration activity in vitro. As shown in Figure 5i,j, MFG-E8 interference significantly inhibited hypoxia-induced cell migration, whereas MFG-E8 silencing in normoxic conditions resulted in a weaker induction trend.

3.9 | Role of MFG-E8 silencing in AKT phosphorylation and cyclin D1 alterations

We next performed western blots to assess the levels of phosphorylated AKT (P-AKT) and cyclin D1 in lysates from PASMCs that were seeded in 6 cm-cell culture dishes, were transfected with MFG-E8 or negative control siRNA, and were cultured in hypoxic or normoxic (2% or 21% oxygen for 24 hr, respectively) conditions (Figure 6). Hypoxia increased the expression of P-AKT and cyclin D1 while pretreatment with MFG-E8 siRNA significantly eliminated these effects. Under normoxic conditions, cell interference targeting MFG-E8 caused an apparent decrease in P-AKT and a trend of decreasing cyclin D1 expression.

4 | DISCUSSION

Our data provide the first evidence for the role of MFG-E8 in the development of hypoxia-induced PH. Herein, we showed that levels of MFG-E8 expression increased in lungs, main pulmonary arteries and plasma in mice exposed to hypoxia; in accordance with the in vivo findings, MFG-E8 in the serum of PH patients and cultured human PASMCs by hypoxic stimuli also exhibited a higher expression (Figures 2 and 3). Mice deficient in the *MFG-E8* gene (Figure 1) showed a modest but still significant response to hypoxia stimulation, as evidenced by elevated PAT/PET, decreased RVSP, attenuated RV hypertrophy and vascular remodeling relative to wild-type mice exposed to hypoxia (Figure 4). Hypoxia accelerated PASMC cell cycle progression, proliferation, and migration, whereas MFG-E8 silencing partially diminished these effects (Figure 5), which might be attributed to alterations in the P-AKT and cyclin D1 pathways (Figure 6).

In this study, we demonstrated that hypoxia could significantly increase MFG-E8 expression both in vivo and in vitro. Previous studies have reported that MFG-E8 is abundantly expressed within vascular cells, such as VSMCs, epithelial cells and macrophages (Ait-Oufella et al., 2007; Bagnato et al., 2007; Beauchamp et al., 2003); furthermore, Beauchamp et al. (2003) confirmed that MFG-E8 was one of the most repressed genes in resting VSMCs. MFG-E8 protein also correlates with cardiovascular remodeling (Fu et al., 2009; Wang et al., 2012) and was found to accumulate in an age-dependent pattern within the intima and media layer of the aorta both in humans and monkeys, which are likely involved in atherosclerosis and vascular thickening (Fu et al., 2009). As shown in our study, hypoxia-induced MFG-E8 protein elevation, especially in VSMCs, was closely related to pulmonary vascular remodeling. Another interesting result is that MFG-E8 is significantly elevated in serum from PH patients, plasma from chronically hypoxic mice, and supernatants from hypoxia-exposed human PASMCs; furthermore, a signal peptide sequence in the N-terminus determines whether the protein is secreted

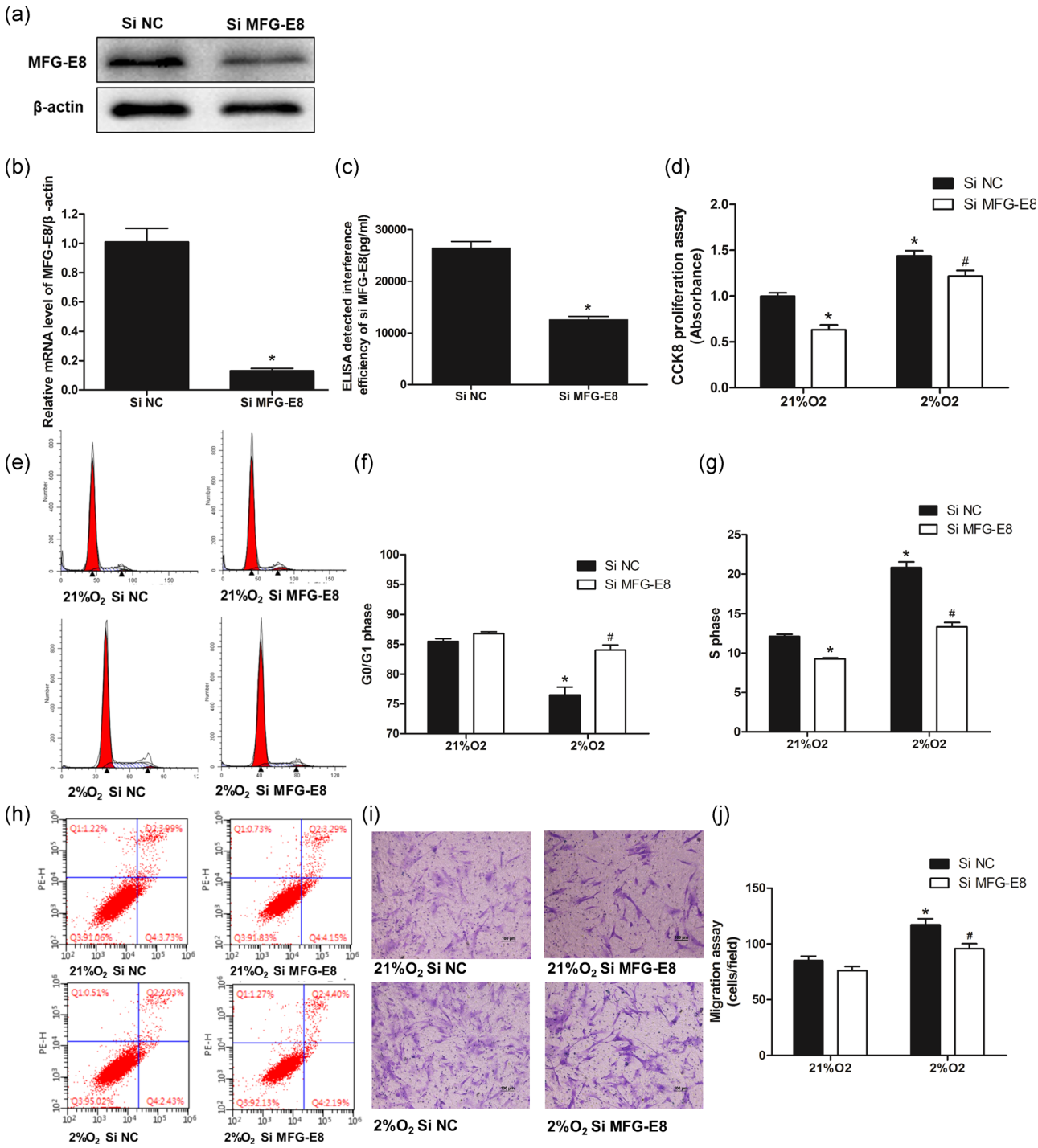

FIGURE 5 Proliferation and cell cycle progression of human PASMCs exposed to hypoxia and/or pretreatment with MFG-E8 silencing. (a–c) Polymerase chain reaction, western blot analysis and ELISA techniques verified the interference efficiency of a small interfering RNA on MFG-E8; $n = 3$, $^{*}p < .05$ compared with the Si NC group. (d) CCK8 proliferation assay of human PASMCs exposed to 2% O_2 for 48 hr and/or pretreatment with Si MFG-E8; $n = 3$. (e) Representative cell cycle analysis images showed cell cycle progression alterations with hypoxia stimulation for 48 hr and/or Si MFG-E8 pretreatment, and the average data of G0/G1 phase (f) and S phase (g); $n = 3$. (h) Representative images of apoptosis analysis showed that neither hypoxia nor MFG-E8 silencing had a significant effect on apoptosis. (i) Representative Transwell assay images showed cell migration alterations with hypoxia and/or MFG-E8 silencing and the average number of migration cells (j); $n = 3$. The results are expressed as the mean ± *SEM*, $^{*}p < 0.05$ compared with the 21% O_2 + Si NC group, and $^{\#}p < .05$ compared with the 2% O_2+Si NC group. CCK8, cell counting kit-8; ELISA, enzyme-linked immunosorbent assay; MFG-E8, milk fat globule-EGF factor 8; NC, negative control; PASMC, pulmonary artery smooth muscle cell

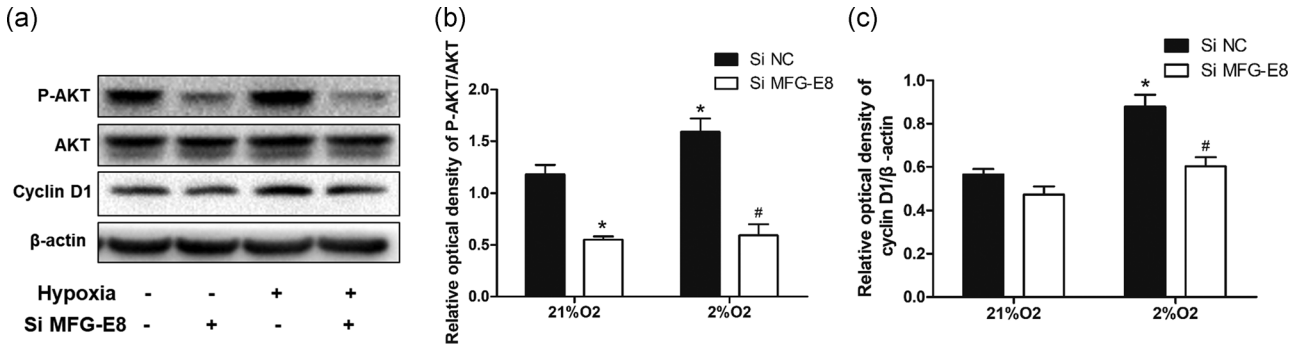

FIGURE 6 Alteration of cyclin D1 and AKT phosphorylation with exposure to hypoxia and/or pretreatment of MFG-E8 silencing. (a) Representative western blot images showed signaling pathway protein alterations in human PASMCs. (b) The ratio of phosphorylated AKT to AKT (P-AKT/AKT) increased after chronic hypoxia, which was attenuated by using MFG-E8 silencing. (c) The cell cycle-related protein cyclin D1 showed changes after exposure to 2% O_2 and/or stimulation with MFG-E8 silencing; $n = 3$. The results are expressed as the mean ± *SEM*, $^{*}p < .05$ compared with the 21% O_2 + Si NC group, and $^{\#}p < .05$ compared with the 2% O_2+Si NC group. AKT, protein kinase B; MFG-E8, milk fat globule-EGF factor 8; NC, negative control; PASMC, pulmonary artery smooth muscle cell

(Aziz et al., 2011; Hanayama et al., 2002), although the structure in humans and murine differs to a certain degree, and the specific mechanism remains unclear. Based on our results, we present the hypothesis that the increased levels of MFG-E8 could serve as a clinically relevant PH biomarker, and more investigations are still needed to prove this possibility.

Mice exposed to chronic hypoxia develop stable PH and RV hypertrophy (Chen et al., 2014; Stenmark et al., 2006). In our study, two methods were performed to evaluate the pulmonary hemodynamics in mice, which reflected increased pulmonary vascular resistance in the chronically hypoxic animals. In chronic PH, RV remodeling may represent an adaptive response to preserve RV contractility because of the increasing afterload. Hypertrophy and hyperplasia of the medial layer is a characteristic pathological feature of vascular remodeling (Stenmark et al., 2006). The results in the hypoxia groups demonstrated that these changes were consistent with previous reports. MFG-E8 has been found to play roles in vascular diseases, and previous studies (Fu et al., 2009; Wang et al., 2012) demonstrated a higher expression within the aortic wall with age. In the meantime, MFG-E8 was thought to colocalize with α-smooth muscle actin, a marker of VSMCs, and functioned in promoting VSMC invasion and proliferation. Our study indicated that the absence of the *MFG-E8* gene could reduce the development of PH. In hypoxia-induced PH, elevated pulmonary vascular resistance is mainly caused by vasoconstriction and vascular remodeling, whereas vascular remodeling (unlike vasoconstriction) becomes increasingly important with time (Pak, Aldashev, Welsh, & Peacock, 2007). Whether MFG-E8 affects vasoconstriction in the PH formation process is valuable for further study. Pulmonary vascular remodeling is mainly due to medial wall thickening through VSMC proliferation. However, other pathological changes are also involved, such as muscularization of small arterioles, VSMC migration, intima proliferation, and ECM deposition (Bloodworth, West, & Merryman, 2015; Pak et al., 2007; Stenmark et al., 2006). The in vivo and in vitro experimental results demonstrated that MFG-E8 deficiency alleviated the pulmonary vascular medial thickness as well as the distal arteriole muscularization, which led to the mitigation of PH. Earlier studies detected abundant MFG-E8 localized to the ECM within the valve hinge, where it might play a role in clearing apoptotic cells (Angel et al., 2011). Similarly, we also observed abnormal ECM deposition in hypoxia-induced PH, which could be inhibited by *MFG-E8* knock-out. There are still some limitations in the present study as we could not directly show MFG-E8 expression in lung tissues because of staining difficulty and the inability to use mice MFG-E8 antibodies in IHC experiments. In addition, we tried to explore MFG-E8 roles in human pulmonary artery endothelial cells (HPAEC) and did not detect apparent changes in HPAEC apoptosis or proliferation following MFG-E8 interference. It is also worth mentioning that the lack of MFG-E8 did not completely offset the hemodynamics and pathological changes seen with PH, which indicates that it is not a sole determinant of the disease.

It is acknowledged that hypoxia stimulates cell proliferation by accelerating DNA synthesis and promoting the mitosis phases of the cell cycle (Wei et al., 2016; Zhang et al., 2014). Our present study showed consistent changes in cell proliferation and cell cycle progression after exposure to hypoxia. We demonstrated that hypoxia stimulated the elevation of MFG-E8 in PASMCs and the cell culture supernatants, while MFG-E8 silencing partially inhibited cell cycle progression at the G0/G1-to-S-phase transition, thus inhibiting cell proliferation. Furthermore, apoptosis analysis indicated that neither hypoxia nor MFG-E8 siRNA transfection affected PASMC apoptosis, which provided supplementary evidence that changes in PASMC numbers were due to cell cycle alterations rather than apoptosis. As mentioned earlier, pulmonary artery remodeling also involved the migration of VSMCs induced by hypoxic stimulation. Finally, we used a migration assay to explore the influence of MFG-E8 on PASMCs and found that MFG-E8 silencing inhibited cell migration.

Previous studies have explored the correlation between MFG-E8 and cell proliferation as well as cell migration. Carrascosa et al. (2012) demonstrated that MFG-E8 promoted cell proliferation and

promoted the expression of cyclin D1/D3 in immortalized mammary epithelial cells, which contributed to the development of mammary carcinoma. MFG-E8 was also found to promote colonic epithelial cell proliferation in vitro, whereas siRNA targeting of α(v)-integrin could inhibit this effect (Kusunoki et al., 2015). Wang et al. (2012) concluded that treatment with recombinant human MFG-E8 facilitated VSMC cell cycle progression and proliferation via integrin signaling, while MFG-E8 silencing could alleviate this influence. A study by Fu et al. (2009) showed that treatment with MFG-E8 or silencing MFG-E8 significantly increased or decreased the invasive capability of VSMCs. In this experiment, we observed similar roles for MFG-E8 towards human PASMCs, suggesting that MFG-E8 contributed to the regulation of PASMC, which might also validate its contribution to pulmonary vascular remodeling observed in a murine PH model. This process presumably involves integrin signaling pathways, given that previous studies suggested that integrins are putative MFG-E8 receptors in many kinds of cells (Kusunoki et al., 2015; Wang et al., 2012; Yang et al., 2011).

Herein, we preliminarily explored the downstream signal transduction alteration with the process of MFG-E8 intervention. Both p-AKT and cyclin D1 were increased following exposure to hypoxia, while MFG-E8 interference significantly suppressed these changes; these observations indicate that MFG-E8 influenced the activation of the P-AKT and cyclin D1 pathways.

AKT phosphorylation has been reported to be involved in the regulation of cell cycle progression, cell proliferation and migration in PASMCs (Goncharova et al., 2002; Guan et al., 2017; Kato & Sherr, 1993; Liu & Fanburg, 2006; Sun, Ramchandran, Chen, Yang, & Raj, 2016). Meanwhile, the cyclin family, including D cyclins, together with CDK, plays important roles in the cell cycle. As a regulatory subunit of CDK4/6, cyclin D1 is indispensable for promoting the G1/S-phase transition and cell proliferation (Andersen, Graversen, Fedosov, Petersen, & Rasmussen, 2000; Dong, Sui, Sugimoto, Tai, & Tokuda, 2001). MFG-E8 mediates integrin signal transduction by recognizing integrin sequences (Jinushi et al., 2008; Liu & Fanburg, 2006; Sun et al., 2016; Taylor, Couto, Scallan, Ceriani, & Peterson, 1997). Previous studies reported that MFG-E8 could enhance tumorigenicity and metastatic seeding of melanoma through AKT- and Twist-dependent signaling by coordinating αvβ3 integrin (Jinushi et al., 2008). In a murine model of postischemic neovascularization, MFG-E8 promoted vascular endothelial growth factor (VEGF)-dependent AKT phosphorylation and blood vessel growth via interactions with αvβ3 and αvβ5 integrins (Silvestre et al., 2005). Our experiments indicated an activation of P-AKT and cyclin D1 in MFG-E8-mediated cell cycle proliferation and migration, which may be mediated by integrin receptors in PASMCs. Furthermore, MFG-E8 silencing in an in vitro study affected cell cycle transitions and cell remodeling in normoxic conditions. In the in vivo study, neither systemic blood pressure nor RVSP showed significant differences between wild-type and MFG-E8-deficient mice when exposed to normoxia. This might be due to regulatory and compensatory mechanisms in vivo, which once again supports the possibility that MFG-E8 might act in concert with other regulatory factors during the development of PH.

In conclusion, our study demonstrates that MFG-E8 is overexpressed in the hypoxia-induced mouse model of PH, and the absence of the *MFG-E8* gene attenuated pulmonary artery pressure and vascular remodeling. Similarly, the MFG-E8 protein also increases in patients with chronic PH, and consistent results are found in human PASMCs that are exposed to hypoxia. Furthermore, MFG-E8 silencing can partially inhibit proliferation, migration and cell cycle progression. The possible mechanisms may involve the interaction between MFG-E8 and the p-Akt/cyclin D1 pathway. Finally, our study highlights the fact that MFG-E8 might be a potential therapeutic target or a biomarker for PH, and its clinical value is worthy of further study.

ACKNOWLEDGMENTS

This study was supported by the National Natural Science Foundation of China (Nos. 81973986, 81570033, 81370145), the National Key Basic Research And Development program (973 Program, No. 20l5CB553403), and the National Key R&D Program of China (Nos. 2016YFC1304500, 2018YFC1311900).

CONFLICT OF INTERESTS

The authors declare that there are no conflict of interests.

AUTHOR CONTRIBUTIONS

Jungang Xie, Jun Wang, and Jixing Wu contributed to the conception and design of this study; Jun Wang and Jixing Wu performed most of the experiments; Xianying Zhu and Jinkun Chen took part in mouse and cell culture experiments; Jun Wang, Jixing Wu, Xianying Zhu, Jinkun Chen, Jianping Zhao, Yongjian Xu, and Jungang Xie were involved in analysis and discussion of the data. Jun Wang, Jixing Wu, and Jungang Xie drafted the manuscript. All authors gave final approval of the version to be submitted.

DATA AVAILABILITY STATEMENT

The data used to support the findings of this study are available from the corresponding author upon request.

ORCID

Jun Wang http://orcid.org/0000-0001-5658-7769
Jixing Wu http://orcid.org/0000-0001-8361-2114
Jungang Xie http://orcid.org/0000-0001-9037-3027

REFERENCES

Ait-Oufella, H., Kinugawa, K., Zoll, J., Simon, T., Boddaert, J., Heeneman, S., … Mallat, Z. (2007). Lactadherin deficiency leads to apoptotic cell accumulation and accelerated atherosclerosis in mice. *Circulation*, *115*(16), 2168–2177. https://doi.org/10.1161/CIRCULATIONAHA.106.662080

Andersen, M. H., Graversen, H., Fedosov, S. N., Petersen, T. E., & Rasmussen, J. T. (2000). Functional analyses of two cellular binding domains of bovine lactadherin. *Biochemistry*, *39*(20), 6200–6206. https://doi.org/10.1021/bi992221r

Angel, P. M., Nusinow, D., Brown, C. B., Violette, K., Barnett, J. V., Zhang, B., … Caprioli, R. M. (2011). Networked-based characterization of extracellular matrix proteins from adult mouse pulmonary and

aortic valves. *Journal of Proteome Research*, *10*(2), 812–823. https://doi.org/10.1021/pr1009806

Arias-Stella, J., & Saldana, M. (1963). The terminal portion of the pulmonary arterial tree in people native to high altitudes. *Circulation*, *28*, 915–925. https://doi.org/10.1161/01.cir.28.5.915

Aziz, M., Jacob, A., Matsuda, A., & Wang, P. (2011). Review: Milk fat globule-EGF factor 8 expression, function and plausible signal transduction in resolving inflammation. *Apoptosis*, *16*(11), 1077–1086. https://doi.org/10.1007/s10495-011-0630-0

Bagnato, C., Thumar, J., Mayya, V., Hwang, S. I., Zebroski, H., Claffey, K. P., … Han, D. K. (2007). Proteomics analysis of human coronary atherosclerotic plaque: A feasibility study of direct tissue proteomics by liquid chromatography and tandem mass spectrometry. *Molecular & Cellular Proteomics*, *6*(6), 1088–1102. https://doi.org/10.1074/mcp.M600259-MCP200

Ball, M. K., Waypa, G. B., Mungai, P. T., Nielsen, J. M., Czech, L., Dudley, V. J., … Schumacker, P. T. (2014). Regulation of hypoxia-induced pulmonary hypertension by vascular smooth muscle hypoxia-inducible factor-1alpha. *American Journal of Respiratory and Critical Care Medicine*, *189*(3), 314–324. https://doi.org/10.1164/rccm.201302-0302OC

Barman, S. A., Li, X., Haigh, S., Kondrikov, D., Mahboubi, K., Bordan, Z., … Fulton, D. J. R. (2019). Galectin-3 is expressed in vascular smooth muscle cells and promotes pulmonary hypertension through changes in proliferation, apoptosis, and fibrosis. *American Journal of Physiology: Lung Cellular and Molecular Physiology*, *316*(5), L784–L797. https://doi.org/10.1152/ajplung.00186.2018

Beauchamp, N. J., van Achterberg, T. A., Engelse, M. A., Pannekoek, H., & de Vries, C. J. (2003). Gene expression profiling of resting and activated vascular smooth muscle cells by serial analysis of gene expression and clustering analysis. *Genomics*, *82*(3), 288–299. https://doi.org/10.1016/s0888-7543(03)00127-7

Beloiartsev, A., da Gloria Rodrigues-Machado, M., Zhou, G. L., Tan, T. C., Zazzeron, L., Tainsh, R. E., … Zapol, W. M. (2015). Pulmonary hypertension after prolonged hypoxic exposure in mice with a congenital deficiency of Cyp2j. *American Journal of Respiratory Cell and Molecular Biology*, *52*(5), 563–570. https://doi.org/10.1165/rcmb.2013-0482OC

Blissenbach, B., Nakas, C. T., Kronke, M., Geiser, T., Merz, T. M., & Pichler Hefti, J. (2018). Hypoxia-induced changes in plasma micro-RNAs correlate with pulmonary artery pressure at high altitude. *American Journal of Physiology: Lung Cellular and Molecular Physiology*, *314*(1), L157–L164. https://doi.org/10.1152/ajplung.00146.2017

Bloodworth, N. C., West, J. D., & Merryman, W. D. (2015). Microvessel mechanobiology in pulmonary arterial hypertension: Cause and effect. *Hypertension*, *65*(3), 483–489. https://doi.org/10.1161/HYPERTENSIONAHA.114.04652

Bogaard, H. J., Abe, K., Vonk Noordegraaf, A., & Voelkel, N. F. (2009). The right ventricle under pressure: Cellular and molecular mechanisms of right-heart failure in pulmonary hypertension. *Chest*, *135*(3), 794–804. https://doi.org/10.1378/chest.08-0492

Carrascosa, C., Obula, R. G., Missiaglia, E., Lehr, H. A., Delorenzi, M., Frattini, M., … Mariotti, A. (2012). MFG-E8/lactadherin regulates cyclins D1/D3 expression and enhances the tumorigenic potential of mammary epithelial cells. *Oncogene*, *31*(12), 1521–1532. https://doi.org/10.1038/onc.2011.356

Chen, J., Tang, H., Sysol, J. R., Moreno-Vinasco, L., Shioura, K. M., Chen, T., … Machado, R. F. (2014). The sphingosine kinase 1/sphingosine-1-phosphate pathway in pulmonary arterial hypertension. *American Journal of Respiratory and Critical Care Medicine*, *190*(9), 1032–1043. https://doi.org/10.1164/rccm.201401-0121OC

Chu, Y., Xiangli, X., & Xiao, W. (2015). Regulatory T cells protect against hypoxia-induced pulmonary arterial hypertension in mice. *Molecular Medicine Reports*, *11*(4), 3181–3187. https://doi.org/10.3892/mmr.2014.3106

Dong, Y., Sui, L., Sugimoto, K., Tai, Y., & Tokuda, M. (2001). Cyclin D1-CDK4 complex, a possible critical factor for cell proliferation and prognosis in laryngeal squamous cell carcinomas. *International Journal of Cancer*, *95*(4), 209–215. https://doi.org/10.1002/1097-0215(20010720)95:4<209::aid-ijc1036>3.0.co;2-r

Fu, Z., Wang, M., Gucek, M., Zhang, J., Wu, J., Jiang, L., … Van Eyk, J. E. (2009). Milk fat globule protein epidermal growth factor-8: A pivotal relay element within the angiotensin II and monocyte chemoattractant protein-1 signaling cascade mediating vascular smooth muscle cells invasion. *Circulation Research*, *104*(12), 1337–1346. https://doi.org/10.1161/CIRCRESAHA.108.187088

Goncharova, E. A., Ammit, A. J., Irani, C., Carroll, R. G., Eszterhas, A. J., Panettieri, R. A., & Krymskaya, V. P. (2002). PI3K is required for proliferation and migration of human pulmonary vascular smooth muscle cells. *American Journal of Physiology: Lung Cellular and Molecular Physiology*, *283*(2), L354–L363. https://doi.org/10.1152/ajplung.00010.2002

Guan, Z., Shen, L., Liang, H., Yu, H., Hei, B., Meng, X., & Yang, L. (2017). Resveratrol inhibits hypoxia-induced proliferation and migration of pulmonary artery vascular smooth muscle cells by inhibiting the phosphoinositide 3-kinase/protein kinase B signaling pathway. *Molecular Medicine Reports*, *16*(2), 1653–1660. https://doi.org/10.3892/mmr.2017.6814

Hanayama, R., Tanaka, M., Miwa, K., Shinohara, A., Iwamatsu, A., & Nagata, S. (2002). Identification of a factor that links apoptotic cells to phagocytes. *Nature*, *417*(6885), 182–187. https://doi.org/10.1038/417182a

Hanayama, R., Tanaka, M., Miyasaka, K., Aozasa, K., Koike, M., Uchiyama, Y., & Nagata, S. (2004). Autoimmune disease and impaired uptake of apoptotic cells in MFG-E8-deficient mice. *Science*, *304*(5674), 1147–1150. https://doi.org/10.1126/science.1094359

Hu, C. J., Poth, J. M., Zhang, H., Flockton, A., Laux, A., Kumar, S., … Stenmark, K. R. (2019). Suppression of HIF2 signalling attenuates the initiation of hypoxia-induced pulmonary hypertension. *European Respiratory Journal*, *54*(6), 1900378. https://doi.org/10.1183/13993003.00378-2019

Huang, W., Wu, J., Yang, H., Xiong, Y., Jiang, R., Cui, T., & Ye, D. (2017). Milk fat globule-EGF factor 8 suppresses the aberrant immune response of systemic lupus erythematosus-derived neutrophils and associated tissue damage. *Cell Death and Differentiation*, *24*(2), 263–275. https://doi.org/10.1038/cdd.2016.115

Jeffery, T. K., & Wanstall, J. C. (2001). Pulmonary vascular remodeling: A target for therapeutic intervention in pulmonary hypertension. *Pharmacology and Therapeutics*, *92*(1), 1–20. https://doi.org/10.1016/s0163-7258(01)00157-7

Jinushi, M., Nakazaki, Y., Carrasco, D. R., Draganov, D., Souders, N., Johnson, M., … Dranoff, G. (2008). Milk fat globule EGF-8 promotes melanoma progression through coordinated Akt and twist signaling in the tumor microenvironment. *Cancer Research*, *68*(21), 8889–8898. https://doi.org/10.1158/0008-5472.CAN-08-2147

Joppa, P., Petrasova, D., Stancak, B., & Tkacova, R. (2006). Systemic inflammation in patients with COPD and pulmonary hypertension. *Chest*, *130*(2), 326–333. https://doi.org/10.1378/chest.130.2.326

Kato, J. Y., & Sherr, C. J. (1993). Inhibition of granulocyte differentiation by G1 cyclins D2 and D3 but not D1. *Proceedings of the National Academy of Sciences of the United States of America*, *90*(24), 11513–11517. https://doi.org/10.1073/pnas.90.24.11513

Kusunoki, R., Ishihara, S., Tada, Y., Oka, A., Sonoyama, H., Fukuba, N., … Kinoshita, Y. (2015). Role of milk fat globule-epidermal growth factor 8 in colonic inflammation and carcinogenesis. *Journal of Gastroenterology*, *50*(8), 862–875. https://doi.org/10.1007/s00535-014-1036-x

Li, B. Y., Li, X. L., Cai, Q., Gao, H. Q., Cheng, M., Zhang, J. H., … Zhou, R. H. (2011). Induction of lactadherin mediates the apoptosis of endothelial cells in response to advanced glycation end products and protective effects of grape seed procyanidin B2 and resveratrol. *Apoptosis*, *16*(7), 732–745. https://doi.org/10.1007/s10495-011-0602-4

Li, Q., Wang, J., Zhu, X., Zeng, Z., Wu, X., Xu, Y., … Yu, J. (2017). Dihydromyricetin prevents monocrotaline-induced pulmonary arterial hypertension in rats. *Biomedicine and Pharmacotherapy*, *96*, 825–833. https://doi.org/10.1016/j.biopha.2017.10.007

Lin, Y. P., Hsu, M. E., Chiou, Y. Y., Hsu, H. Y., Tsai, H. C., Peng, Y. J., … Lin, C. H. (2010). Comparative proteomic analysis of rat aorta in a subtotal nephrectomy model. *Proteomics*, *10*(13), 2429–2443. https://doi.org/10.1002/pmic.200800658

Liu, Y., & Fanburg, B. L. (2006). Serotonin-induced growth of pulmonary artery smooth muscle requires activation of phosphatidylinositol 3-kinase/serine-threonine protein kinase B/mammalian target of rapamycin/p70 ribosomal S6 kinase 1. *American Journal of Respiratory Cell and Molecular Biology*, *34*(2), 182–191. https://doi.org/10.1165/rcmb.2005-0163OC

Naeije, R. (2005). Pulmonary hypertension and right heart failure in chronic obstructive pulmonary disease. *Proceedings of the American Thoracic Society*, *2*(1), 20–22. https://doi.org/10.1513/pats.200407-037MS

Novoyatleva, T., Kojonazarov, B., Owczarek, A., Veeroju, S., Rai, N., Henneke, I., … Schermuly, R. T. (2019). Evidence for the fucoidan/P-selectin axis as a therapeutic target in hypoxia-induced pulmonary hypertension. *American Journal of Respiratory and Critical Care Medicine*, *199*(11), 1407–1420. https://doi.org/10.1164/rccm.201806-1170OC

Olsson, K. M., Olle, S., Fuge, J., Welte, T., Hoeper, M. M., Lerch, C., … Schiffer, L. (2016). CXCL13 in idiopathic pulmonary arterial hypertension and chronic thromboembolic pulmonary hypertension. *Respiratory Research*, *17*, 21. https://doi.org/10.1186/s12931-016-0336-5

Oshima, K., Aoki, N., Kato, T., Kitajima, K., & Matsuda, T. (2002). Secretion of a peripheral membrane protein, MFG-E8, as a complex with membrane vesicles. *European Journal of Biochemistry*, *269*(4), 1209–1218. https://doi.org/10.1046/j.1432-1033.2002.02758.x

Pak, O., Aldashev, A., Welsh, D., & Peacock, A. (2007). The effects of hypoxia on the cells of the pulmonary vasculature. *European Respiratory Journal*, *30*(2), 364–372. https://doi.org/10.1183/09031936.00128706

Raymond, A., Ensslin, M. A., & Shur, B. D. (2009). SED1/MFG-E8: A bi-motif protein that orchestrates diverse cellular interactions. *Journal of Cellular Biochemistry*, *106*(6), 957–966. https://doi.org/10.1002/jcb.22076

Rohm, I., Grun, K., Muller, L. M., Kretzschmar, D., Fritzenwanger, M., Yilmaz, A., … Franz, M. (2017). Increased serum levels of fetal tenascin-C variants in patients with pulmonary hypertension: novel biomarkers reflecting vascular remodeling and right ventricular dysfunction? *International Journal of Molecular Sciences*, *18*(11), 239–249. https://doi.org/10.3390/ijms18112371

Sajkov, D., & McEvoy, R. D. (2009). Obstructive sleep apnea and pulmonary hypertension. *Progress in Cardiovascular Diseases*, *51*(5), 363–370. https://doi.org/10.1016/j.pcad.2008.06.001

Shur, B. D., Ensslin, M. A., & Rodeheffer, C. (2004). SED1 function during mammalian sperm-egg adhesion. *Current Opinion in Cell Biology*, *16*(5), 477–485. https://doi.org/10.1016/j.ceb.2004.07.005

Silvestre, J. S., Thery, C., Hamard, G., Boddaert, J., Aguilar, B., Delcayre, A., … Mallat, Z. (2005). Lactadherin promotes VEGF-dependent neovascularization. *Nature Medicine*, *11*(5), 499–506. https://doi.org/10.1038/nm1233

Simonneau, G., Gatzoulis, M. A., Adatia, I., Celermajer, D., Denton, C., Ghofrani, A., … Souza, R. (2013). Updated clinical classification of pulmonary hypertension. *Journal of the American College of Cardiology*, *62*(25 Suppl.), D34–D41. https://doi.org/10.1016/j.jacc.2013.10.029

Song, X. W., Zou, L. L., Cui, L., Li, S. H., Qin, Y. W., Zhao, X. X., & Jing, Q. (2018). Plasma miR-451 with echocardiography serves as a diagnostic reference for pulmonary hypertension. *Acta Pharmacologica Sinica*, *39*(7), 1208–1216. https://doi.org/10.1038/aps.2018.39

Stenmark, K. R., Fagan, K. A., & Frid, M. G. (2006). Hypoxia-induced pulmonary vascular remodeling: Cellular and molecular mechanisms. *Circulation Research*, *99*(7), 675–691. https://doi.org/10.1161/01.RES.0000243584.45145.3f

Strange, C., & Highland, K. B. (2005). Pulmonary hypertension in interstitial lung disease. *Current Opinion in Pulomnary Medicine*, *11*(5), 452–455. https://doi.org/10.1097/01.mcp.0000174250.38188.6d

Sun, M., Ramchandran, R., Chen, J., Yang, Q., & Raj, J. U. (2016). Smooth muscle insulin-like growth factor-1 mediates hypoxia-induced pulmonary hypertension in neonatal mice. *American Journal of Respiratory Cell and Molecular Biology*, *55*(6), 779–791. https://doi.org/10.1165/rcmb.2015-0388OC

Taylor, M. R., Couto, J. R., Scallan, C. D., Ceriani, R. L., & Peterson, J. A. (1997). Lactadherin (formerly BA46), a membrane-associated glycoprotein expressed in human milk and breast carcinomas, promotes Arg-Gly-Asp (RGD)-dependent cell adhesion. *DNA and Cell Biology*, *16*(7), 861–869. https://doi.org/10.1089/dna.1997.16.861

Udjus, C., Cero, F. T., Halvorsen, B., Behmen, D., Carlson, C. R., Bendiksen, B. A., … Larsen, K. O. (2019). Caspase-1 induces smooth muscle cell growth in hypoxia-induced pulmonary hypertension. *American Journal of Physiology: Lung Cellular and Molecular Physiology*, *316*(6), L999–L1012. https://doi.org/10.1152/ajplung.00322.2018

van Suylen, R. J., Aartsen, W. M., Smits, J. F., & Daemen, M. J. (2001). Dissociation of pulmonary vascular remodeling and right ventricular pressure in tissue angiotensin-converting enzyme-deficient mice under conditions of chronic alveolar hypoxia. *American Journal of Respiratory and Critical Care Medicine*, *163*(5), 1241–1245. https://doi.org/10.1164/ajrccm.163.5.2003144

Wang, M., Fu, Z., Wu, J., Zhang, J., Jiang, L., Khazan, B., … Lakatta, E. G. (2012). MFG-E8 activates proliferation of vascular smooth muscle cells via integrin signaling. *Aging Cell*, *11*(3), 500–508. https://doi.org/10.1111/j.1474-9726.2012.00813.x

Wei, C., Li, H. Z., Wang, Y. H., Peng, X., Shao, H. J., Li, H. X., … Xu, C. Q. (2016). Exogenous spermine inhibits the proliferation of human pulmonary artery smooth muscle cells caused by chemically-induced hypoxia via the suppression of the ERK1/2- and PI3K/AKT-associated pathways. *International Journal of Molecular Medicine*, *37*(1), 39–46. https://doi.org/10.3892/ijmm.2015.2408

Xiao, Y., Gong, D., & Wang, W. (2013). Soluble JAGGED1 inhibits pulmonary hypertension by attenuating notch signaling. *Arteriosclerosis, Thrombosis, and Vascular Biology*, *33*(12), 2733–2739. https://doi.org/10.1161/ATVBAHA.113.302062

Yang, C., Hayashida, T., Forster, N., Li, C., Shen, D., Maheswaran, S., … Schmidt, E. V. (2011). The integrin alpha(v)beta(3-5) ligand MFG-E8 is a p63/p73 target gene in triple-negative breast cancers but exhibits suppressive functions in ER(+) and erbB2(+) breast cancers. *Cancer Research*, *71*(3), 937–945. https://doi.org/10.1158/0008-5472.CAN-10-1471

Zhang, H., Gong, Y., Wang, Z., Jiang, L., Chen, R., Fan, X., … Kong, X. (2014). Apelin inhibits the proliferation and migration of rat PASMCs via the activation of PI3K/Akt/mTOR signal and the inhibition of autophagy under hypoxia. *Journal of Cellular and Molecular Medicine*, *18*(3), 542–553. https://doi.org/10.1111/jcmm.12208

SUPPORTING INFORMATION

Additional supporting information may be found online in the Supporting Information section.

How to cite this article: Wang J, Wu J, Zhu X, et al. Absence of the MFG-E8 gene prevents hypoxia-induced pulmonary hypertension in mice. *J Cell Physiol*. 2021;236:587–600. https://doi.org/10.1002/jcp.29885